A Barycentric Coordinate-Based Approach to Formation Control Under Directed and Switching Sensing Graphs

Tingrui Han, Zhiyun Lin, *Senior Member, IEEE*, Ronghao Zheng, and Minyue Fu, *Fellow, IEEE*

***Abstract*—This paper investigates two formation control problems for a leader–follower network in 3-D. One is called the formation marching control problem, the objective of which is to steer the agents to maintain a target formation shape while moving with the synchronized velocity. The other one is called the formation rotating control problem, whose goal is to drive the agents to rotate around a common axis with a target formation. For the above two problems, we consider directed and switching sensing topologies while the communication is assumed to be bidirectional and switching. We develop approaches utilizing barycentric coordinates toward these two problems. Local control laws and graphical conditions are acquired to ensure global convergence in both scenarios.**

***Index Terms*—Barycentric coordinate, formation control, leader–follower network, switching sensing graph.**

I. Introduction

FORMATION control has attracted much interest due to its tremendous engineering applications [1]. Recently, many works have been reported on this topic such as [2]–[4], some of which focus on swarm and flocking [5]–[7], containment control [8]–[10] and achieving a given pattern [11]–[16].

In the light of the kind of sensed variables for formation control, the reference [17] divides the existing literature into three categories, that is, position-, displacement-, and distance-based control, which are outlined as follows.

Manuscript received October 28, 2016; revised January 21, 2017; accepted March 9, 2017. Date of publication March 31, 2017; date of current version March 15, 2018. This work was supported by the National Natural Science Foundation of China under Grant 61673344 and Grant 61503335. This paper was recommended by Associate Editor X.-M. Sun. *(Corresponding author: Zhiyun Lin.)*

T. Han is with the College of Electrical Engineering, Zhejiang University, Hangzhou 310027, China (e-mail: hantingrui@zju.edu.cn).

Z. Lin is with the College of Electrical Engineering, Zhejiang University, Hangzhou 310027, China, and also with the School of Automation, Hangzhou Dianzi University, Hangzhou 310027, China (e-mail: linz@zju.edu.cn).

R. Zheng is with the College of Electrical Engineering, Zhejiang University, Hangzhou 310027, China, and also with the Zhejiang Province Marine Renewable Energy Electrical Equipment and System Technology Research Laboratory, Zhejiang University, Hangzhou 310027, China (e-mail: rzheng@zju.edu.cn).

M. Fu is with the School of Electrical Engineering and Computer Science, University of Newcastle, Callaghan, NSW 2308, Australia, and also with Zhejiang University, Hangzhou 310027, China (e-mail: minyue.fu@newcastle.edu.au).

Color versions of one or more of the figures in this paper are available online at http://ieeexplore.ieee.org.

Digital Object Identifier 10.1109/TCYB.2017.2684461

A. Position-Based Control

Each agent is able to sense its position in a global coordinate system, then it is controlled to reach a target formation, which is prescribed by the desired position in the global coordinate system.

B. Displacement-Based Control

Each agent is able to sense the relative positions of its neighbors in a global coordinate system, then it is controlled to reach a target formation, which is prescribed by the desired displacements in the global coordinate system. Thus, displacement-based control requires that the axes of the agents' local coordinate systems should have the same orientations.

C. Distance-Based Control

Each agent is able to sense the relative positions of its neighbors in its own local coordinate system, then it is controlled to reach a target formation, which is prescribed by the desired interagent distances. This indicates that the agents do not need to have a common orientation of local coordinate systems.

Most recently, an approach based on barycentric coordinates for formation shape control is introduced in [18]–[20] which can be executed in local frames. This is because the barycentric coordinate is a geometric notion characterizing the relative positions of a point with respect to other points in absence of the global frame [21]. We sum up the barycentric-coordinate-based control as below.

D. Barycentric-Coordinate-Based Control

Each agent is able to sense the relative positions of its neighbors in its own local coordinate system like the one for distance-based control, and is controlled to reach a target formation, which is prescribed by the desired barycentric coordinates of every agent with respect to its neighbors.

As a comparison, the barycentric-coordinate-based control requires less advanced sensing capability than position-based and displacement-based control, and needs less interactions among agents than distance-based control, as shown in Fig. 1.

Along the recent research based on barycentric coordinates, [18] and [19] adopt complex barycentric coordinates to solve the formation control problem in 2-D. Later on, the work [20] implements real barycentric coordinates to settle

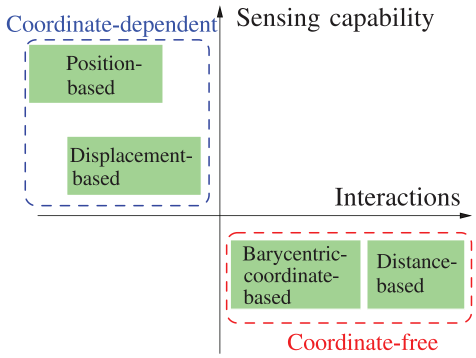

Fig. 1. Sensing capability versus interactions.

the formation control problem in higher dimensions. In the existing works mentioned above, [18] and [20] both assume that the sensing topology is fixed. However, discussing switching topologies becomes more attractive due to the existence of sensing failure. From this perspective, [19] considers switching topologies, but only a peculiar switching signal is discussed, that is, an agent can either sense all its neighbors or sense none of them. Besides, the developed controller in [19] is not fully distributed because the computation of some parameters involves the knowledge concerning the whole network. Motivated by this need, our previous work [22] studies the formation control problem over switching topologies for a leader–follower network under the premise that the followers lie in the convex hull spanned by the leaders in the target configuration. The controller in [22] is fully distributed, however, a convexity assumption is imposed on the desired formation shape, which limits the applicability.

In this paper, we aim to remove the convexity assumption in [22] by allowing the interaction weights to be negative, which makes the setup general enough to include any desired formation pattern. According to the practical demand in engineering, two formation control problems are investigated in this paper, namely, formation marching control problem and formation rotating control problem. The task of formation marching is to drive the agents to realize any target formation while moving with the synchronized velocity. Formation marching can be often seen in UAVs maneuvering and target detecting. The goal of formation rotating is to steer the agents to move around a common axis with any specified formation shape. Formation rotating control can find many useful applications such as satellites and spacecrafts flying around the earth and circular mobile sensor networks collecting measurements [23]–[25]. References [26], [27] study formation rotating control problems, where Lin *et al.* utilized the Lyapunov-based approach, which, however, is only workable for undirected and fixed topologies. In this paper, although considering directed and switching scenarios, we can also show that the formation rotating control can be achieved by utilizing the barycentric-coordinate-based control.

To overcome the difficulties induced by switching topologies for the above two problems, a communication graph is introduced and an auxiliary state information is exchanged, with which a fully distributed control law is developed for each problem. To show global convergence toward the desired formation shape under switching topologies, the idea of persistent excitation is adopted. With this method, the graphical conditions are obtained to ensure that all the agents are able to globally converge to the desired formation. As the first attempt to develop the barycentric-coordinate-based control for general switching topologies, single-integrator kinematic model for each agent is considered in this paper. With the purpose of extending the results to the second-order cases or more complex agent dynamics, one way is to take advantage of the backstepping philosophy, that is to say, design the acceleration input such that the velocity signal in the second-order case converges to the designed velocity input in the paper [20].

The rest of this paper is organized as follows. We review some preliminaries about graph theory in Section II and two formation control problems are formulated in Section III. We develop a control law for the formation marching control and prove its convergence in Section IV. Moreover, a control law is proposed for the formation rotating control and its stability is analyzed in Section V. Three simulation examples are presented in Section VI to validate our theoretical results. Section VII concludes this paper and points out possible future research.

Notation: $\mathbb{R}$ represents the set of real numbers. Denote $\mathbf{1}_n$ the n-dimensional vector of ones and I_n the identity matrix of order n. The symbol $\otimes$ is the Kronecker product.

II. Preliminaries

A *directed graph* is defined by $\mathcal{G} = (\mathcal{V}, \mathcal{E})$, which consists of a vertex set $\mathcal{V}$ of elements called *nodes* and a set $\mathcal{E} \subset \mathcal{V} \times \mathcal{V}$ of ordered pairs of nodes called *edges*. For each node $i \in \mathcal{V}$, denote $\mathcal{N}_i^+ = \{j \in \mathcal{V} : (j, i) \in \mathcal{E}\}$ the set of its *in-neighbors* while $\mathcal{N}_i^- = \{h \in \mathcal{V} : (i, h) \in \mathcal{E}\}$ represents the set of its *out-neighbors*.

An $n \times n$ Laplacian matrix L corresponding to a directed graph $\mathcal{G}$ is defined as

$$L(i,j) = \begin{cases} -w_{ij} & \text{if } i \neq j \text{ and } j \in \mathcal{N}_i^+ \\ 0 & \text{if } i \neq j \text{ and } j \notin \mathcal{N}_i^+ \\ \sum\limits_{k \in \mathcal{N}_i^+} w_{ik} & \text{if } i = j \end{cases}$$

where $L(i, j)$ is the (i, j)-th entry of L and $w_{ij} \in \mathbb{R}\backslash\{0\}$ is called the weight on edge (j, i).

For a directed graph $\mathcal{G} = (\mathcal{V}, \mathcal{E})$, a node v is said to be k*-reachable* from a subset $\mathcal{R} \subset \mathcal{V}$ if there exists a path from a node in $\mathcal{R}$ to node v after deleting any $k - 1$ nodes except node v.

A *time-varying graph* is defined as $\mathcal{G}(t) = (\mathcal{V}, \mathcal{E}(t))$, representing a graph with its edge set changing over time. The *union graph* $\mathcal{G}([t_1, t_2])$ is defined by

$$\mathcal{G}([t_1, t_2]) = \left(\mathcal{V}, \bigcup_{t \in [t_1, t_2]} \mathcal{E}(t)\right).$$

For a time-varying graph $\mathcal{G}(t)$, a node v is called *jointly* k*-reachable* from a set $\mathcal{R}$ if there exists $T > 0$ such that for all t, node v is k-reachable from $\mathcal{R}$ in the union graph $\mathcal{G}([t, t+T))$, where T is called the *period*.

For a graph $\mathcal{G} = (\mathcal{V}, \mathcal{E})$, a *spanning k-tree* of $\mathcal{G}$ rooted at $\mathcal{R} = \{r_1, r_2, \dots, r_k\} \subset \mathcal{V}$ is a subgraph of $\mathcal{G}$ such that:

1) every node $r \in \mathcal{R}$ has no in-neighbor;
2) every node $v \notin \mathcal{R}$ has k in-neighbors;
3) every node $v \notin \mathcal{R}$ is k-reachable from $\mathcal{R}$.

For a graph $\mathcal{G} = (\mathcal{V}, \mathcal{E})$, a *spanning k-forest* of $\mathcal{G}$ rooted at $\mathcal{R} = \{r_1, r_2, \dots, r_m\} \subset \mathcal{V}$ with $m \geq k$ is a subgraph of $\mathcal{G}$ such that:

1) every node $r \in \mathcal{R}$ has no in-neighbor;
2) every node $v \notin \mathcal{R}$ has k in-neighbors;
3) every node $v \notin \mathcal{R}$ is k-reachable from $\mathcal{R}$.

Remark 1: We would like to mention that a spanning k-tree has exactly k roots while a spanning k-forest may have more than k roots.

A *configuration* in $\mathbb{R}^3$ of n nodes is defined by their coordinates in $\mathbb{R}^3$, denoted as $p = [p_1^\intercal, \dots, p_n^\intercal]^\intercal \in \mathbb{R}^{3n}$, where $p_i \in \mathbb{R}^3$ for $i = 1, \dots, n$. Moreover, we say p is *generic* if the coordinates $p_1, \dots, p_n$ do not satisfy any nontrivial algebraic equation with integer coefficients [28].

A *framework* in $\mathbb{R}^3$ is a graph $\mathcal{G}$ equipped with a configuration p, denoted as $(\mathcal{G}, p)$. Two frameworks $(\mathcal{G}, p)$ and $(\mathcal{G}, q)$ are called *similar* if

$$p_i - p_j = \gamma A\big(q_i - q_j\big) \text{ for all } i, j \in \mathcal{V}$$

where $\gamma > 0$ is a scaling factor and A is a unitary matrix.

For a matrix $A \in \mathbb{R}^{n\times n}$, the *associated graph* is defined as $\mathcal{G}(A)$, which has n nodes labeled by $1, \dots, n$, and an edge (j, i) exists if and only if the (i, j)-th entry of A is nonzero.

III. Problem Formulation

In engineering applications, agents may perform marching when maneuvering and searching target. Moveover, in some scenarios, agents may execute circular motions such as flying around a landmark. Thereby, two specific problems toward formation control will be studied in this paper. One of them is called the *formation marching control problem*, the goal of which is to steer the agents to form a target formation shape while moving with the synchronized velocity. The other one is called the *formation rotating control problem*, whose objective is to drive the agents rotating around a common axis with a target formation shape.

Measurements between agents may be unidirectional due to the limit of equipped devices such as cameras which only have a conical field of vision. In addition, measurements may fail sometimes due to severe environment factors. So a more general setup with directed and switching sensing graphs is adopted to model the multiagent systems in this paper.

We consider a leader–follower network of N agents in the three dimensions, where there are m leaders labeled from 1 to m and $N-m$ followers labeled from $m+1$ to N. Define a target configuration $p = [p_l^\intercal, p_f^\intercal]^\intercal \in \mathbb{R}^{3N}$ for all the agents where $p_l = [p_1^\intercal, \dots, p_m^\intercal]^\intercal$ aggregates the states of the leaders while $p_f = [p_{m+1}^\intercal, \dots, p_N^\intercal]^\intercal$ aggregates the states of the followers. Throughout this paper, a vector notation equipped with the subscript l is used to represent the aggregated state for the leaders and likewise f is used for the followers.

Denote the global coordinate system by Σ_g and the agent i's local coordinate system by Σ_i. Let $z_i \in \mathbb{R}^3$ be the 3-D position of agent i in the global frame Σ_g. Moreover, let $z_j^{(i)}$ be the value of agent j's position in agent i's local frame Σ_i, and from now on we use the superscript (i) to represent the value in Σ_i. Let O_i be the origin of Σ_i in Σ_g, that is, $O_i^{(i)} = 0$. Define R_i the rotation matrix from Σ_i to Σ_g, i.e., $z_j - O_i = R_i(z_j^{(i)} - O_i^{(i)}),\ j \in \mathcal{V}$. Furthermore, define R_{ij} the rotation matrix from Σ_j and Σ_i, i.e., $z_j^{(i)} - O_j^{(i)} = R_{ij}(z_j^{(j)} - O_j^{(j)})$.

Suppose each agent is governed by the following dynamics:

$$\dot{z}_i^{(i)}(t) = u_i^{(i)}(t),\ \ i = 1, \dots, N \tag{1}$$

where $u_i^i(t) \in \mathbb{R}^3$ represents the control input of agent i.

The leaders are said to be in a similar formation p_l if their positions satisfy

$$z_i(t_0) = \gamma A p_i + c,\ \ i = 1, \dots, m \tag{2}$$

where $A \in \mathbb{R}^{3\times 3}$ is a unitary matrix, $c \in \mathbb{R}^3$ is a constant vector implying the translation, and $\gamma > 0$ is a scaling factor. We assume in this paper that the leaders are in a similar formation p_l and we concentrate on devising controllers for the followers.

It is assumed that each agent is provided with sensors such as cameras and manages to sense the relative positions of its neighbors in its local frame. A time-varying graph $\bar{\mathcal{G}}(t) = (\mathcal{V}, \bar{\mathcal{E}}(t))$ is adopted to model the *sensing graph*, where $\mathcal{V} = \mathcal{V}_l \cup \mathcal{V}_f$ with $\mathcal{V}_l = \{1, \dots, m\}$ and $\mathcal{V}_f = \{m+1, \dots, N\}$. That is to say, $(j, i) \in \bar{\mathcal{E}}(t)$ indicates that agent i has the ability to sense the relative position of agent j in Σ_i at time t. Let $\bar{\mathcal{N}}_i^+(t)$ be the set of agent i's in-neighbors in graph $\bar{\mathcal{G}}(t)$ and likewise $\bar{\mathcal{N}}_i^-(t)$ denotes the set of agent i's out-neighbors. Note that $j \in \bar{\mathcal{N}}_i^+(t)$ if and only if $(j, i) \in \bar{\mathcal{E}}(t)$.

Moreover, each agent is assumed to equip devices to communicate with other agents. However, the devices implemented for sensing and communication may be different. Thus, We adopt another time-varying graph $\mathcal{H}(t)$ to model the *communication graph*, where an edge (j, i) indicates that agent j can transmit information to agent i. Usually, devices support two-way communication and communication distance is longer than sensing distance, which makes it reasonable to have the following assumption.

Assumption 1: The communication graph $\mathcal{H}(t)$ is bidirectional. Moreover, the communication graph $\mathcal{H}(t)$ contains the sensing graph $\bar{\mathcal{G}}(t)$ as a subgraph at any time t.

Moreover, the following assumptions are also made throughout this paper.

Assumption 2: The target configuration $p = [p_l^\intercal, p_f^\intercal]^\intercal$ is generic.

Assumption 3: Agent i has access to the rotation matrix $R_{ij},\ j \in \bar{\mathcal{N}}_i^+(t)$.

Assumption 4: The interval between any two switching instants satisfies a dwell time condition. That is to say, there exists $\tau_D > 0$ such that

$$t_{i+1} - t_i \geq \tau_D \text{ for all } i = 0, 1, \dots$$

if the sensing graph $\bar{\mathcal{G}}(t)$ switches at $t_0, t_1, t_2, \dots$.

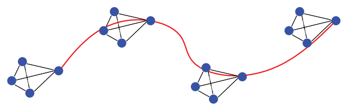

Fig. 2. Simple illustrative example for formation marching.

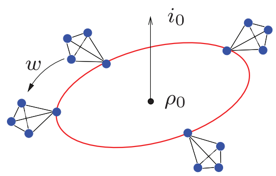

Fig. 3. Simple illustrative example for formation rotating.

A. Formation Marching Control Problem

The objective is to steer all the agents converge to form a similar formation with a common velocity $v_r(t)$. A simple illustrative example for formation marching is given in Fig. 2.

Let the motion of the leaders be governed by

$$\dot{z}_i^{(i)}(t) = v_r^{(i)}(t), \ \ i = 1, \ldots, m \tag{3}$$

where $v_r^{(i)}(t)$ is the common velocity. Assume that each agent i, $i = 1, \ldots, N$, has access to the velocity $v_r^{(i)}(t)$.

Remark 2: For the situation that $v_r^{(i)}(t)$ is only known to a subset of the followers, some techniques can be included to make it possible (see [22]).

For simplicity of analysis, we write (3) in Σ_g as

$$\dot{z}_i(t) = v_r(t), \ \ i = 1, \ldots, m. \tag{4}$$

We next give the precise definition about achieving a similar formation for the formation marching control.

Definition 1: A similar formation $p = [p_l^{\mathsf{T}}, p_f^{\mathsf{T}}]^{\mathsf{T}}$ is said to be globally uniformly asymptotically achieved for the formation marching control problem if for any $\delta > 0$ and for any $\varepsilon > 0$ there exists $T > 0$ such that for any t_0 and for any $z_i(t_0)$ satisfying $\|z_i(t_0) - \gamma A p_i - c\| < \delta, \ i = 1, \ldots, N$

$$(\forall t \geq t_0 + T)(\forall i)\left\| z_i(t) - \gamma A p_i - c - \int_{t_0}^{t} v_r(\tau) d\tau \right\| < \varepsilon \tag{5}$$

where A, c, and γ are determined in (2).

Then we are able to give the description for the formation marching control problem as below. Suppose the leaders are in a similar formation p_l and governed by (4). Given Assumptions 1–4 and relative position measurements $z_j^{(i)} - z_i^{(i)}$ for $j \in \bar{\mathcal{N}}_i^{+}(t)$, design a fully distributed control law $u_i^{(i)}$ for each follower i, and find the corresponding graphical conditions, under which (5) is satisfied.

B. Formation Rotating Control Problem

The objective is to drive all the agents surround a common axis with a similar formation. We use a unit vector $i_0 \in \mathbb{R}^3$ which passes a point $\rho_0 \in \mathbb{R}^3$ to represent this axis, denoted by $i_0(\rho_0)$. That is, all the agents finally move on the circular orbits around $i_0(\rho_0)$ while keeping a desired formation shape. A simple illustrative example for formation rotating is shown in Fig. 3.

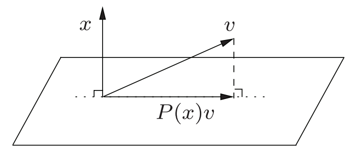

Fig. 4. Geometric explanation for the orthogonal projection operator.

We assume the synchronized angular velocity $\omega = 1$ for simplicity since it follows the same analysis if ω takes other values. Moreover, we introduce a new coordinate system $\Sigma_{i'}$ for each agent i such that the z-axis of $\Sigma_{i'}$ is parallel to i_0. Let $\Sigma_{i'}$ and Σ_i share the common origin. The rotation matrix from Σ_i to $\Sigma_{i'}$ is denoted as $R_{i'i} \in \mathbb{R}^{3\times 3}$, that is, $z_i^{(i')} = R_{i'i} z_i^{(i)}$, where the superscript (i') represents the value in $\Sigma_{i'}$.

Remark 3: Notice that we do not define the x-axis and y-axis of $\Sigma_{i'}$ explicitly, so $R_{i'i}$ can take different values. However, it does not affect the analysis and conclusions.

The next assumption is required to achieve formation rotating.

Assumption 5: Each leader i manages to sense the relative position $\rho_0^{(i)} - z_i^{(i)}$ and each agent i has access to the vector $i_0^{(i)}$.

Remark 4: For the situation that the vector $i_0^{(i)}$ is only known to a subset of the agents, $i_0^{(i)}$ can be known to all the agents through communication if Assumption 3 holds.

Let the motion of the leaders be governed by

$$\dot{z}_i^{(i)} = -R_{i'i}^{-1} R\left(\frac{\pi}{2}\right) R_{i'i} P\left(i_0^{(i)}\right)\left(\rho_0^{(i)} - z_i^{(i)}\right), \quad i = 1, \ldots, m \tag{6}$$

where the function $P(x)$ is the orthogonal projection operator on the unit vector x defined by $P(x) = I - xx^{\mathsf{T}}$. Geometrically, $P(x)$ is an orthogonal projection matrix that projects any vector onto the orthogonal compliment of x. See Fig. 4 for an illustration. And $R(\pi/2)$ is attained by the rotation matrix

$$R(\cdot) = \begin{bmatrix} \cos(\cdot) & -\sin(\cdot) & 0 \\ \sin(\cdot) & \cos(\cdot) & 0 \\ 0 & 0 & 1 \end{bmatrix}.$$

Denote $R_{i'}$ the rotation matrix from $\Sigma_{i'}$ to Σ_g, that is, $z_j - O_{i'} = R_{i'}(z_j^{(i')} - O_{i'}^{(i')})$, $j \in \mathcal{V}$. Then we can write the dynamics (6) in the global frame Σ_g as

$$\dot{z}_i = -R_{i'}^{-1} R\left(\frac{\pi}{2}\right) R_{i'} P(i_0)(\rho_0 - z_i), \ \ i = 1, \ldots, m. \tag{7}$$

Remark 5: Note that the dynamics (7) indicates that every leader moves surrounding $i_0(\rho_0)$ anticlockwise (looking along the negative direction of i_0) with the angular velocity $\omega = 1$.

We next give the formal definition about achieving the similar formation for the formation rotating control problem.

Definition 2: A similar formation $p = [p_l^{\mathsf{T}}, p_f^{\mathsf{T}}]^{\mathsf{T}}$ is said to be globally uniformly asymptotically achieved for the formation rotating control problem if for any $\delta > 0$ and for any $\varepsilon > 0$ there exists $T > 0$ such that for any t_0 and for any $z_i(t_0)$ satisfying $\|z_i(t_0) - \gamma A p_i - c\| < \delta, \ i = 1, \ldots, N$, then it holds that for all $t \geq t_0 + T$

$$\left\| z_i(t) - R_{i'}^{-1} R(t - t_0) R_{i'}(\gamma A p_i + c - \rho_0) - \rho_0 \right\| < \varepsilon \tag{8}$$

where A, c, and γ are determined in (2).

Now, we can give the description for the formation rotating control problem. Suppose that the leaders are already in a similar formation p_l and governed by (6). Given Assumptions 1–5 and relative position measurements $z_j^{(i)} - z_i^{(i)}$ for $j \in \bar{\mathcal{N}}_i^+(t)$, design a fully distributed control law $u_i^{(i)}$ for each follower i, and find the corresponding graphical conditions, under which (8) is satisfied.

IV. Formation Marching Control

In this section, we first focus on designing a fully distributed control law for formation marching control problem. Then more insight behind the ideas of barycentric-coordinate-based control is introduced. At last, we conduct the convergence analysis for the whole leader–follower network under the proposed control law.

A. Distributed Control Law

The basic idea to utilize the barycentric-coordinate-based control is to establish the barycentric coordinate representation for each agent i with respect to its in-neighbors. At least four in-neighbors are necessary to have this representation. Thus, if $|\bar{\mathcal{N}}_i^+(t)| < 4$, then agent i will not make use of the sensed measurements and just abandon them. In term of this mechanism, an *interaction graph* $\mathcal{G}(t) = (\mathcal{V}, \mathcal{E}(t))$ is constructed depending on which in-neighbors are chosen to interact. Denote $\mathcal{N}_i^+(t)$ the set of agent i's in-neighbors in $\mathcal{G}(t)$ and $\mathcal{N}_i^-(t)$ the set of agent i's out-neighbors. In other words, if $|\bar{\mathcal{N}}_i^+(t)| < 4$, then $\mathcal{N}_i^+(t) = \emptyset$. Otherwise, $\mathcal{N}_i^+(t) = \bar{\mathcal{N}}_i^+(t)$.

We develop the following linear switching control law for each follower $i = m+1, \ldots, N$:

$$\begin{cases} \dot{\xi}_i = -\frac{1}{2}\xi_i - \sum_{j\in\mathcal{N}_i^+(t)} k_{ij}(t)\left(z_j^{(i)} - z_i^{(i)}\right) \\ \dot{z}_i^{(i)} = v_r^{(i)}(t) - \sum_{j\in\mathcal{N}_i^+(t)} k_{ij}(t)\xi_i + \sum_{j\in\mathcal{N}_i^-(t)} k_{ji}(t)R_{ij}\xi_j \end{cases} \tag{9}$$

where ξ_i is an auxiliary state with the values for the leaders being zero, i.e., $\xi_1 = \cdots = \xi_m = 0$, and $k_{ij}(t) \in \mathbb{R}\backslash\{0\}$ is the weight associated with edge (j, i) in $\mathcal{G}(t)$ satisfying

$$\sum_{j\in\mathcal{N}_i^+(t)} k_{ij}(t)(p_j - p_i) = 0. \tag{10}$$

Remark 6: By Assumption 4 and the design of $k_{ij}(t)$s we know that $k_{ij}(t)$s are piecewise constant.

Remark 7: Notice that computing $k_{ij}(t)$s from (10) is distributed and can be carried out by each agent i with known p_i and p_j $(j \in \mathcal{N}_i^+(t))$. Moreover, $z_j^{(i)} - z_i^{(i)}$ $(j \in \mathcal{N}_i^+(t))$ is acquired by onboard sensors and $k_{ji}R_{ij}\xi_j$ $(j \in \mathcal{N}_i^-(t))$ is attained through communication. Thus, the controller (9) is fully distributed, namely, all the parameters can be determined in a distributed way. An illustration of information flow including sensing and communication is displayed in Fig. 5, where the solid lines represent the measurements obtained by sensors and the dashed lines stand for the information exchange through communication.

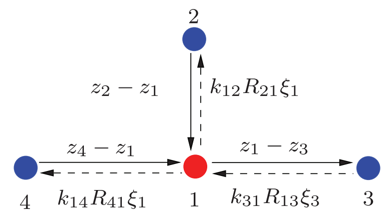

Fig. 5. Illustration of information flow including sensing and communication for (9).

Now we define $\zeta_i = R_i\xi_i$ and it is obtained that

$$\begin{aligned}\zeta_i = R_i\dot{\xi}_i &= -\frac{1}{2}R_i\xi_i - \sum_{j\in\mathcal{N}_i^+(t)} k_{ij}(t)R_i\left(z_j^{(i)} - z_i^{(i)}\right) \\ &= -\frac{1}{2}\zeta_i - \sum_{j\in\mathcal{N}_i^+(t)} k_{ij}(t)\left(z_j - z_i\right)\end{aligned}$$

and we also have

$$\begin{aligned}\dot{z}_i &= R_i\dot{z}_i^{(i)} \\ &= R_iv_r^{(i)}(t) - \sum_{j\in\mathcal{N}_i^+(t)} k_{ij}(t)R_i\xi_i + \sum_{j\in\mathcal{N}_i^-(t)} k_{ji}(t)R_iR_{ij}\xi_j \\ &= v_r(t) - \sum_{j\in\mathcal{N}_i^+(t)} k_{ij}(t)\zeta_i + \sum_{j\in\mathcal{N}_i^-(t)} k_{ji}(t)\zeta_j.\end{aligned}$$

Hence, the system (9) can be written in the global frame

$$\begin{cases} \dot{\zeta}_i = -\frac{1}{2}\zeta_i - \sum_{j\in\mathcal{N}_i^+(t)} k_{ij}(t)\left(z_j - z_i\right), \\ \dot{z}_i = v_r(t) - \sum_{j\in\mathcal{N}_i^+(t)} k_{ij}(t)\zeta_i + \sum_{j\in\mathcal{N}_i^-(t)} k_{ji}(t)\zeta_j. \end{cases} \tag{11}$$

Denote $L(t)$ the Laplacian of $\mathcal{G}(t)$ with the weights $k_{ij}(t)$s computed by (10), which has the following structure:

$$L(t) = \left[\begin{array}{c|c} 0_{m\times m} & 0_{m\times(N-m)} \\ \hline L_{lf}(t) & L_{ff}(t) \end{array}\right]. \tag{12}$$

According to the design of $k_{ij}(t)$s, $L(t)$ satisfies

$$(L(t)\otimes I_3)p = 0 \text{ and } L(t)\mathbf{1} = 0. \tag{13}$$

B. Barycentric Coordinate-Based Idea

In this section, we aim to provide more insight behind the ideas of barycentric-coordinate-based control. To give clearer explanation about the basic idea, we consider a fixed graph $\mathcal{G}$.

The barycentric coordinate is a geometric notion characterizing the relative position of a point with respect to other points. In the three dimensions, at least four other points are needed for a point to have a barycentric coordinate representation. Recall (10)

$$\sum_{j\in\mathcal{N}_i^+} k_{ij}\left(p_j - p_i\right) = 0$$

where p_i has a barycentric coordinate representation with respect to its in-neighbors, that is

$$\sum_{j\in\mathcal{N}_i^+} k_{ij}p_i = \sum_{j\in\mathcal{N}_i^+} k_{ij}p_j.$$

The basic idea of barycentric-coordinate-based control is that each follower drives $\sum_{j\in\mathcal{N}_i^+} k_{ij}(z_j - z_i)$ to zero. The following lemma shows that $(L \otimes I_3)z = 0$ and $\det(L_{ff}) \neq 0$ indicate that the followers reach the target formation.

Lemma 1: Suppose that the leaders are in a similar formation. If $(L \otimes I_3)z = 0$ and $\det(L_{ff}) \neq 0$, then

$$z_f = (I_{N-m} \otimes \gamma A)p_f + \mathbf{1}_{N-m} \otimes \left(c + \int_{t_0}^{t} v_r(\tau)d\tau\right).$$

Proof: Note that $(L \otimes I_3)p = 0$ and $L\mathbf{1} = 0$. Then we have

$$\begin{aligned}(L \otimes I_3)&\left[(I_N \otimes \gamma A)p + \mathbf{1}_N \otimes (c + \int_{t_0}^{t} v_r(\tau)d\tau)\right]\\ &= (L \otimes I_3)(I_N \otimes \gamma A)p = (L \otimes \gamma A)p\\ &= (I_N \otimes \gamma A)(L(t) \otimes I_3)p = 0.\end{aligned}$$

Since $\det(L_{ff}) \neq 0$, z_f solved from $(L \otimes I_3)z = 0$ is unique. Therefore, the conclusion follows. ■

The next lemma provides the fact that if the number of the leaders is less than 4, then L_{ff} must be singular. Before that, we denote by $\mathcal{L}(\mathcal{G})$ the set of all Laplacian matrices with nonzero weights on the edges in $\mathcal{G}$. It is true that for any matrix $L \in \mathcal{L}(\mathcal{G})$, we have $L\mathbf{1} = 0$. For a set $\mathcal{R} \subset \mathcal{V}$, let $L_{\mathcal{R}}$ be the sub-matrix constructed from L by removing the rows and columns corresponding to $\mathcal{R}$.

Lemma 2: Consider a graph $\mathcal{G} = (\mathcal{V}, \mathcal{E})$ with n nodes and generic $\xi, \zeta, \eta \in \mathbb{R}^n$. Given the set $\mathcal{R} = \{r_1, \ldots, r_m\}$, if $m < 4$, then $\det(L_{\mathcal{R}}) = 0$ for any $L \in \{L \in \mathcal{L}(\mathcal{G}) : L\xi = 0, L\zeta = 0, L\eta = 0\}$.

The proof of Lemma 2 is given in the Appendix. The next theorem presents the relationship between the nonsingularity of L_{ff} and the topology connectivity of $\mathcal{G}$.

Theorem 1: Consider a graph $\mathcal{G} = (\mathcal{V}, \mathcal{E})$ with n nodes and generic $\xi, \zeta, \eta \in \mathbb{R}^n$. Given the set $\mathcal{R} = \{r_1, \ldots, r_m\}$ with $m \geq 4$, the following statements are equivalent.

1) Every node in $\mathcal{V}\backslash\mathcal{R}$ is 4-reachable from $\mathcal{R}$.
2) For almost all[1] $L \in \{L \in \mathcal{L}(\mathcal{G}) : L\xi = 0, L\zeta = 0, L\eta = 0\}$, all the principal minors of $L_{\mathcal{R}}$ are nonzero.

The proof of Theorem 1 is stated in the Appendix.

Remark 8: The basic idea of displacement-based control is to run consensus on $z_i - p_i$ for every agent where p_i is the target configuration. Thus, displacement-based control asks for the common orientation of all the local frames due to the presence of p_i. However, the main idea of barycentric-coordinate-based control is to drive $\sum_{j\in\mathcal{N}_i^+} k_{ij}(z_j - z_i)$ to zero, where p is only used to compute k_{ij}. As a consequence, barycentric-coordinate-based control makes it possible to devise coordinate-free control laws. Moreover, Lemma 1 shows that the leaders are able to reconfigure the formation shape while the followers can only act as dummies, which cannot be achieved by displacement-based control.

Remark 9: Distance-based control utilizes nonlinear local constraints, which only guarantees local asymptotic convergence and is nonrobust with respect to distance mismatches [30]. Global convergence based on distance-based control is only available for some special graphs [31] while barycentric-coordinate-based control makes global convergence possible for more general graphs by using linear distributed control laws. Moreover, barycentric-coordinate-based control requires less edges to achieve a target formation shape than distance-based control. Specifically, for distance-based control, the underlying graph needs to be globally rigid, which requires more links between leaders and followers compared with the graphical condition presented in Theorem 1.

C. Stability Analysis

In this section, we provide the convergence analysis for the whole system under the controller (11) for the formation marching control problem.

Define z and ζ the aggregated vectors of all z_is and ζ_is, respectively. Under the distributed control law (11), the overall closed-loop system can be written as

$$\begin{bmatrix}\dot{z}\\ \dot{\zeta}\end{bmatrix} = \left(\begin{bmatrix}0 & -H(t)\\ L(t) & -U\end{bmatrix} \otimes I_3\right)\begin{bmatrix}z\\ \zeta\end{bmatrix} + \begin{bmatrix}\mathbf{1}_N\\ 0\end{bmatrix} \otimes v_r \tag{14}$$

where

$$H(t) = \begin{bmatrix}0 & 0\\ 0 & L_{ff}^{\top}(t)\end{bmatrix},\ U = \begin{bmatrix}0 & 0\\ 0 & \frac{1}{2}I_{N-m}\end{bmatrix}.$$

The next theorem provides graphical conditions to ensure global convergence for the whole system.

Theorem 2: Under control law (11), for almost all chosen weights, a similar formation $p = [p_l^{\top}, p_f^{\top}]^{\top}$ can be globally uniformly asymptotically achieved for the formation marching control problem if the following two conditions hold.

1) Every follower is jointly 4-reachable from $\mathcal{V}_l$ in the interaction graph $\mathcal{G}(t)$ with period T.
2) For any t and any follower i, there exists $t_i' \in [t, t+T)$ such that $\mathcal{N}_i^{\mathcal{F}} \subseteq \mathcal{N}_i^+(t_i')$, where $\mathcal{F}$ is a spanning 4-forest rooted at $\mathcal{V}_l$ in the union graph $\mathcal{G}([t, t+T))$ and $\mathcal{N}_i^{\mathcal{F}}$ represents the set of is in-neighbors in $\mathcal{F}$.

Before presenting technical proof for Theorem 2, we develop the next lemma and introduce a lemma summarized from [32] which provides a persistently exciting condition ensuring exponential stability for switching systems.

Given generic $\xi, \zeta, \eta \in \mathbb{R}^n$, denote $\Omega_i(\mathcal{F}) = \{L(i,:) : L \in \mathcal{L}(\mathcal{F}), L\xi = 0, L\zeta = 0, L\eta = 0\}$ and $\Omega_i(\mathcal{G}) = \{L(i,:) : L \in \mathcal{L}(\mathcal{G}), L\xi = 0, L\zeta = 0, L\eta = 0\}$, where $L(i,:)$ represents the i-th row of L.

Lemma 3: Consider a graph $\mathcal{G} = (\mathcal{V}, \mathcal{E})$ with n nodes and a set $\mathcal{R} = \{r_1, \ldots, r_m\}$ where $m \geq 4$. Suppose that every node in $\mathcal{V}\backslash\mathcal{R}$ is 4-reachable from $\mathcal{R}$ and $\mathcal{F}$ is a spanning 4-forest rooted at $\mathcal{R}$. If for any node i it holds that Θ_i is a subspace satisfying $\Omega_i(\mathcal{F}) \subset \Theta_i \subset \Omega_i(\mathcal{G})$, then for almost all[2] L formed by $L(i,:) \in \Theta_i$, all principal minors of $L_{\mathcal{R}}$ are nonzero.

We postpone the proof of Lemma 3 to the Appendix.

Denote the set $T_\Delta = \{t_i\}$ of elements in $[0, \infty)$, where there exists a positive Δ such that for all $t_i, t_j \in T_\Delta$ ($t_i \neq t_j$), it holds that $|t_i - t_j| \geq \Delta$. Furthermore, let Γ be the set of functions

[1]The phrase "for almost all" means "for all values except those in some proper algebraic variety with Lebesgue measure zero" [29].

[2]The phrase "for almost all L" can be understood by "for almost all k_{ij}s used to construct L."

$v(\cdot)$ defined on $[0, \infty)$, where for every $v(\cdot)$ there exists T_Δ such that:

1) $v(t)$ and $\dot{v}(t)$ are continuous and bounded on $[0, \infty)\backslash T_\Delta$;
2) $v(t)$ and $\dot{v}(t)$ have finite limits as $t \to t_i^+$ and $t \to t_i^-$, where $t_i \in T_\Delta$.

Lemma 4 [32]: Let $V(\cdot) : \mathbb{R}_+ \to \mathbb{R}^{n\times r}$ be a regulated matrix function (one-sided limits exist for all $t \in \mathbb{R}_+$), and satisfy for some positive δ and α_1, and all $t \in \mathbb{R}_+$

$$\int_t^{t+\delta} \|V(\tau)\|^2 d\tau < \alpha_1. \tag{15}$$

Suppose also that the entries of $V(\cdot)$ lie in Γ. Let M be a real constant $n \times n$ matrix with $M + M^\mathsf{T} = -I_n$ and let B be a real constant $n \times r$ matrix with rank r. Then

$$\dot{x} = \begin{bmatrix} 0 & -VB^\mathsf{T} \\ BV^\mathsf{T} & M \end{bmatrix} x \tag{16}$$

is exponentially stable if and only if for some positive δ and α_2, and all $t \in \mathbb{R}_+$

$$\int_t^{t+\delta} V(\tau)V^\mathsf{T}(\tau)d\tau \geq \alpha_2 I. \tag{17}$$

Lemma 5 [33]: Consider m matrices $A_1, \ldots, A_m \in \mathbb{R}^{n\times n}$. If $\mathrm{rank}(A_1 + A_2 + \cdots + A_m) = n$, then the matrix $A_1^\mathsf{T} A_1 + A_2^\mathsf{T} A_2 + \cdots + A_m^\mathsf{T} A_m$ is positive definite.

Proof of Theorem 2: Denote $y = z - \mathbf{1}_N \otimes \int_{t_0}^t v_r(\tau)d\tau$ and the system (14) becomes

$$\begin{bmatrix} \dot{y} \\ \dot{\zeta} \end{bmatrix} = \left(\begin{bmatrix} 0 & -H(t) \\ L(t) & -U \end{bmatrix} \otimes I_3 \right) \begin{bmatrix} y \\ \zeta \end{bmatrix}. \tag{18}$$

Since the fact

$$\begin{aligned}(L(t) \otimes I_3)\big[(I_N \otimes \gamma A)p + \mathbf{1}_N \otimes c\big] \\ = (L(t) \otimes \gamma A)p = (I_N \otimes \gamma A)(L(t) \otimes I_3)p = 0\end{aligned}$$

we get that

$$\begin{cases} y^* = (I_N \otimes \gamma A)p + \mathbf{1}_N \otimes c \\ \zeta^* = 0 \end{cases} \tag{19}$$

is an equilibrium point of system (18), which implies that

$$\begin{cases} z^*(t) = (I_N \otimes \gamma A)p + \mathbf{1}_N \otimes \left(c + \int_{t_0}^t v_r(\tau)d\tau\right) \\ \zeta^* = 0 \end{cases}$$

is an equilibrium solution of system (14).

Recall that the leaders are in a similar formation, that is to say, $y_l(t) = y_l^*$. Apply the coordinate transformation $e_f = y_f - y_f^*$ for the followers and we have

$$\begin{bmatrix} \dot{e}_f \\ \dot{\zeta}_f \end{bmatrix} = \left(\begin{bmatrix} 0 & -L_{ff}^\mathsf{T}(t) \\ L_{ff}(t) & -\frac{1}{2}I_n \end{bmatrix} \otimes I_3 \right) \begin{bmatrix} e_f \\ \zeta_f \end{bmatrix}. \tag{20}$$

Notice that the system (20) can be derived by substituting

$$x = \begin{bmatrix} e_f \\ \zeta_f \end{bmatrix}, M = -\frac{1}{2} I_n \otimes I_3, B = I_n \otimes I_3, \text{ and } V = L_{ff}^\mathsf{T} \otimes I_3$$

into (16) in Lemma 4. In what follows, we prove that all the conditions described in Lemma 4 are satisfied.

Suppose the graph $\mathcal{G}(t)$ switches at $t_0, t_1, t_2, \ldots$. From Assumption 4 we know that $t_{i+1} - t_i \geq \tau_D$ for all $i = 0, 1, 2 \ldots$. Moreover, we are always able to find a $\tau_M > \tau_D$ large enough such that $t_{i+1} - t_i \leq \tau_M$ for all $i = 0, 1, 2, \ldots$. If for some interval $[t_i, t_{i+1})$ there is no such a τ_M, then $[t_i, t_{i+1})$ can be partitioned to satisfy this condition.

Suppose every follower is jointly 4-reachable from $\mathcal{V}_l$. Then there exits $T > 0$ such that every follower is 4-reachable from $\mathcal{V}_l$ in the union graph $\mathcal{G}([t, t + T))$ for all t.

Since $L_{ff}(t)$ is piecewise constant, it is obtained that $L_{ff}(t)$ is regulated. We choose δ as $\delta = T + 2\tau_M$. Since $k_{ij}(t)$s are taken from a finite set, we attain that $\|L_{ff}(t)\|^2$ is uniform upper-bounded, which indicates that there exists a positive α_1 such that for all t, it holds that

$$\int_t^{t+\delta} \|L_{ff}^\mathsf{T}(\tau)\|^2 d\tau < \alpha_1.$$

Therefore, according to Lemma 4, it remains to show that there exists a positive α_3 such that for all t, it holds that

$$\int_t^{t+\delta} L_{ff}^\mathsf{T}(\tau)L_{ff}(\tau)d\tau \geq \alpha_3 I. \tag{21}$$

In the following, we will prove that (21) is satisfied. Considering any t, without loss of generality, denote $t \in (t_{l_1}, t_{l_1+1}]$ and $t + \delta \in [t_{l_2}, t_{l_2+1})$. We let

$$W := \int_t^{t+\delta} L_{ff}^\mathsf{T}(\tau)L_{ff}(\tau)d\tau.$$

Moreover, we define

$$H := L^\mathsf{T}(t_{l_1+1})L(t_{l_1+1}) + \cdots + L^\mathsf{T}(t_{l_2-1})L(t_{l_2-1})$$

and

$$X := L(t_{l_1+1}) + \cdots + L(t_{l_2-1}).$$

Thus, for almost all $L(t)$, the inequality

$$L(t_k)(i, j) \neq 0, \ \ k = l_1 + 1, \ldots, l_2 - 1$$

leads to the fact that $X(i, j) \neq 0$, which implies that

$$\mathcal{G}(X) = \mathcal{G}(L(t_{l_1+1})) \cup \cdots \cup \mathcal{G}(L(t_{l_2-1})).$$

Furthermore, it is also known that

$$\mathcal{G}([t_{l_1+1}, t_{l_2})) = \mathcal{G}(L(t_{l_1+1})) \cup \cdots \cup \mathcal{G}(L(t_{l_2-1})) = \mathcal{G}(X).$$

Since $(X \otimes I_3)p = 0$ and $X\mathbf{1}_N = 0$, the matrix X can be also regarded as a Laplacian matrix with the following structure:

$$\left[\begin{array}{c|c} * & * \\ \hline * & X_{ff} \end{array}\right]$$

where $X_{ff} = L_{ff}(t_{l_1+1}) + \cdots + L_{ff}(t_{l_2-1})$.

Due to $t_{l_1+1} - t \leq \tau_M$ and $t + \delta - t_{l_2} \leq \tau_M$, we have $t_{l_2} - t_{l_1+1} \geq T$. Hence, every follower is 4-reachable from $\mathcal{V}_l$ in the union graph $\mathcal{G}([t_{l_1+1}, t_{l_2}))$. According to the second graphical condition in Theorem 2, $\mathcal{G}([t_{l_1+1}, t_{l_2}))$ has a spanning 4-forest $\mathcal{F}$ and $\mathcal{N}_i^{\mathcal{F}} \subseteq \mathcal{N}_i(t')$ for some $t' \in [t_{l_1+1}, t_{l_2})$. Thus, we can infer that for each i, the set $\{X(i, :)\}$ induced by all possible Xs satisfies $\{L(i, :) : L \in \mathcal{L}(\mathcal{F}), (L \otimes I_3)p = 0\} \subset \{X(i, :)\}$. Then it follows from Lemma 3 that:

$$\det\big(X_{ff}\big) \neq 0. \tag{22}$$

Now we come to look at H which has the following form:

$$\left[\begin{array}{c|c} * & * \\ \hline * & H_{ff} \end{array}\right]$$

where

$$H_{ff} = L_{ff}^{\mathsf{T}}(t_{l_1+1})L_{ff}(t_{l_1+1}) + \cdots + L_{ff}^{\mathsf{T}}(t_{l_2-1})L_{ff}(t_{l_2-1}).$$

By Lemma 5 and the inequality (22), it is certain that

$$\det\big(H_{ff}\big) \neq 0.$$

Together with the fact that H_{ff} is positive semi-definite, it can be obtained that H_{ff} is positive definite.

Note that the matrix W can be written as

$$\begin{aligned} W = {} & L_{ff}^{\mathsf{T}}(t_{l_1})L_{ff}(t_{l_1})(t_{l_1+1} - t) \\ & + L_{ff}^{\mathsf{T}}(t_{l_1+1})L_{ff}(t_{l_1+1})(t_{l_1+2} - t_{l_1+1}) + \cdots \\ & + L_{ff}^{\mathsf{T}}(t_{l_2-1})L_{ff}(t_{l_2-1})(t_{l_2} - t_{l_2-1}) \\ & + L_{ff}^{\mathsf{T}}(t_{l_2})L_{ff}(t_{l_2})(t + \delta - t_{l_2}). \end{aligned}$$

Since we have shown that H_{ff} is positive definite, in implies that for any vector $v \neq 0$ it holds that $v^{\mathsf{T}}H_{ff}v > 0$. So it can be easily obtained that for any vector $v \neq 0$, it holds that $v^{\mathsf{T}}Wv > 0$. Thus, W is also positive definite. To prove (21) holds, it is required to show that the smallest eigenvalue of W is uniform lower bounded on t.

Notice that $L_{ff}(t)$s are taken from a finite set. Moreover, the number of switches during $[t, t+\delta)$ is not more than $\lceil \delta/\tau_D \rceil$, which indicates that H is also taken from a finite set. Since for all $i = 0, 1, 2, \ldots,$ it holds that $\tau_D \leq t_{i+1} - t_i \leq \tau_M$. Moreover, it is also known that $0 \leq t_{l_1+1} - t \leq \tau_M$ and $0 \leq t + \delta - t_{l_2} \leq \tau_M$. Hence, we can infer from the expression of W that there exists $\alpha_3 > 0$ such that for all t

$$W \geq \alpha_3 I.$$

Thus, the state $[e_f^{\mathsf{T}}, \zeta_f^{\mathsf{T}}]^{\mathsf{T}}$ will converge to zero exponentially, which equivalently indicates that z_f converges to z_f^* exponentially. Therefore, the conclusion follows. ■

Remark 10: Considering static topologies, it follows from Theorem 1 that the graphical condition that every follower is 4-reachable from $\mathcal{V}_l$ is necessary for global convergence under (9). Moreover, we can infer from Theorem 2 that this graphical condition is also sufficient since for static topologies condition (1) implies condition (2). To sum up, 4-reachability is necessary and sufficient for static topologies to ensure convergence. For switching topologies, Theorem 2 shows that the graph does not need to satisfy 4-reachability all the time. It only requires that the union graph satisfies the conditions frequently, which is much milder.

V. Formation Rotating Control

In this section, we first develop a fully distributed control law for the formation rotating control problem and then analyze its stability.

A. Distributed Control Law

In this section, a fully distributed control law is proposed for the formation rotating control problem.

Let η_i be the estimation of $\rho_0^{(i)} - z_i^{(i)}$ for every agent i. Indeed, for the leaders, we have $\eta_i = \rho_0^{(i)} - z_i^{(i)}$. Then we give the following estimation algorithm for each follower i:

$$\dot{\eta}_i = -\dot{z}_i^{(i)} + \sum_{j\in\mathcal{N}_i^+(t)} (z_j^{(i)} - z_i^{(i)} + R_{ij}\eta_j - \eta_i). \tag{23}$$

Define $x_i = R_i\eta_i$ and we obtain that

$$\begin{aligned} \dot{x}_i = R_i\dot{\eta}_i &= -R_i\dot{z}_i^{(i)} + \sum_{j\in\mathcal{N}_i^+(t)} R_i\Big(z_j^{(i)} - z_i^{(i)} + R_{ij}\eta_j - \eta_i\Big) \\ &= -\dot{z}_i + \sum_{j\in\mathcal{N}_i^+(t)} \big(z_j - z_i + R_iR_{ij}\eta_j - x_i\big) \\ &= -\dot{z}_i + \sum_{j\in\mathcal{N}_i^+(t)} \big(z_j - z_i + x_j - x_i\big). \end{aligned}$$

Thus, the algorithm (23) can be written in Σ_g as

$$\dot{x}_i = -\dot{z}_i + \sum_{j\in\mathcal{N}_i^+(t)} \big(z_j - z_i + x_j - x_i\big). \tag{24}$$

Lemma 6: Under (24), for each follower i, x_i globally uniformly asymptotically converges to $\rho_0 - z_i$ if and only if every follower is jointly reachable from the leaders.

Proof: Let $y_i = x_i - (\rho_0 - z_i)$ and it is known that $y_i = 0$ for $i = 1, \ldots, m$. Moreover, we attain that

$$\dot{y}_i = \dot{x}_i + \dot{z}_i = \sum_{j\in\mathcal{N}_i^+(t)} \big(y_j - y_i\big),\ \ i = m+1, \ldots, N. \tag{25}$$

Notice that (25) is the well-known consensus algorithm with the states of the leaders being zero. With the same technique used in the proof of [22, Th. 5.1], we directly obtain that y_i uniformly asymptotically converges to zero if and only if every follower is jointly reachable from the leaders. ■

By the transformation $y_i = x_i - (\rho_0 - z_i)$ we can rewrite the controller (7) as

$$\dot{z}_i = -R_{i'}^{-1}R\Big(\frac{\pi}{2}\Big)R_{i'}P(i_0)x_i,\ \ i = 1, \ldots, m. \tag{26}$$

Next, we are able to propose the controller for the followers:

$$\left\{\begin{aligned} \dot{z}_i^{(i)} &= -R_{i'i}^{-1}R\Big(\frac{\pi}{2}\Big)R_{i'i}P\Big(i_0^{(i)}\Big)\eta_i - \sum_{j\in\mathcal{N}_i^+(t)} k_{ij}(t)\xi_i \\ &\quad + \sum_{j\in\mathcal{N}_i^-(t)} k_{ji}(t)R_{ij}\xi_j, \\ \dot{\xi}_i &= -R_{i'i}^{-1}\hat{R}R_{i'i}\xi_i - \frac{1}{2}\xi_i - \sum_{j\in\mathcal{N}_i^+(t)} k_{ij}(t)\Big(z_j^{(i)} - z_i^{(i)}\Big) \end{aligned}\right. \tag{27}$$

where

$$\hat{R} = \begin{bmatrix} 0 & 1 & 0 \\ -1 & 0 & 0 \\ 0 & 0 & 0 \end{bmatrix}$$

and k_{ij}s are designed in the same way as the control law (11).

Define $\zeta_i = R_i\xi_i$ and we derive that

$$\begin{aligned}\dot{\zeta}_i &= R_i\dot{\xi}_i = -R_iR_{i'i}^{-1}\hat{R}R_{i'i}R_i^{-1}R_i\xi_i - \frac{1}{2}\zeta_i \\ &\quad - \sum_{j\in\mathcal{N}_i^+(t)} k_{ij}(t)\big(z_j - z_i\big) \\ &= -R_{i'}^{-1}\hat{R}R_{i'}\zeta_i - \frac{1}{2}\zeta_i - \sum_{j\in\mathcal{N}_i^+(t)} k_{ij}(t)\big(z_j - z_i\big).\end{aligned}$$

Moreover, we also have

$$\begin{aligned}\dot{z}_i = R_i\dot{z}_i^{(i)} &= -R_iR_{i'i}^{-1}R\Big(\frac{\pi}{2}\Big)R_{i'i}P\Big(i_0^{(i)}\Big)\eta_i \\ &\quad - \sum_{j\in\mathcal{N}_i^+(t)} k_{ij}(t)\zeta_i + \sum_{j\in\mathcal{N}_i^-(t)} k_{ji}(t)\zeta_j \\ &= -R_{i'}^{-1}R\Big(\frac{\pi}{2}\Big)R_{i'}P(i_0)x_i \\ &\quad - \sum_{j\in\mathcal{N}_i^+(t)} k_{ij}(t)\zeta_i + \sum_{j\in\mathcal{N}_i^-(t)} k_{ji}(t)\zeta_j.\end{aligned}$$

Hence, the control law (27) can be written in the global coordinate system by

$$\begin{cases}\dot{z}_i = -R_{i'}^{-1}R(\frac{\pi}{2})R_{i'}P(i_0)x_i - \sum_{j\in\mathcal{N}_i^+(t)} k_{ij}(t)\zeta_i \\ \qquad + \sum_{j\in\mathcal{N}_i^-(t)} k_{ji}(t)\zeta_j \\ \dot{\zeta}_i = -R_{i'}^{-1}\hat{R}R_{i'}\zeta_i - \frac{1}{2}\zeta_i - \sum_{j\in\mathcal{N}_i^+(t)} k_{ij}(t)\big(z_j - z_i\big).\end{cases} \tag{28}$$

B. Stability Analysis

In this section, we analyze the convergence of the whole system under the controller (28).

The next theorem presents the same conditions as the ones in Theorem 2 to guarantee global convergence.

Theorem 3: Under control law (28), for almost all chosen weights, a similar formation $p = [p_l^\top, p_f^\top]^\top$ can be globally uniformly asymptotically realized for the formation rotating control problem if the following two conditions hold.

1) Every follower is jointly 4-reachable from $\mathcal{V}_l$ in the interaction graph $\mathcal{G}(t)$ with period T.
2) For any t and any follower i, there exists $t_i' \in [t, t+T)$ such that $\mathcal{N}_i^{\mathcal{F}} \subseteq \mathcal{N}_i^+(t_i')$, where $\mathcal{F}$ is a spanning 4-forest in the union graph $\mathcal{G}([t, t+T))$ and $\mathcal{N}_i^{\mathcal{F}}$ represents the set of i's in-neighbors in $\mathcal{F}$.

The proof of Theorem 3 requires a lemma concerning cascade systems.

Lemma 7 [34]: Consider the following nonlinear time-varying system:

$$\dot{x}_1 = f_1(t, x_1) + g(t, x)x_2 \tag{29}$$

$$\dot{x}_2 = f_2(t, x_2) \tag{30}$$

where $x = [x_1^\top, x_2^\top]^\top$. The system (29) and (30) is globally uniformly asymptotically stable if the following conditions are satisfied.

1) For each $r > 0$ there exists $\bar{c}(r) > 0$ such that if $\|x(t_0)\| < r$ then $\|x(t; t_0, x(t_0))\| \le \bar{c}(r)$.
2) System $\dot{x}_1 = f_1(t, x_1)$ is globally uniformly asymptotically stable.
3) System (30) is globally uniformly asymptotically stable.

Proof of Theorem 3: Let

$$\psi_i = R_{i'}^{-1}R(t_0 - t)R_{i'}(z_i - \rho_0) + \rho_0.$$

Then for the leaders, we know that

$$\begin{aligned}\dot{\psi}_i &= R_{i'}^{-1}\dot{R}(t_0 - t)R_{i'}(z_i - \rho_0) + R_{i'}^{-1}R(t_0 - t)R_{i'}\dot{z}_i \\ &= R_{i'}^{-1}\dot{R}(t_0 - t)R_{i'g}(z_i - \rho_0) - R_{i'}^{-1}R(t_0 - t)R\Big(\frac{\pi}{2}\Big)R_{i'}P(i_0)x_i \\ &= R_{i'}^{-1}\begin{bmatrix}-\sin(t - t_0) & \cos(t - t_0) & 0 \\ -\cos(t - t_0) & -\sin(t - t_0) & 0 \\ 0 & 0 & 0\end{bmatrix}\Big(z_i^{(i')} - \rho_0^{(i')}\Big) \\ &\quad + R_{i'}^{-1}\begin{bmatrix}-\sin(t - t_0) & \cos(t - t_0) & 0 \\ -\cos(t - t_0) & -\sin(t - t_0) & 0 \\ 0 & 0 & 1\end{bmatrix}P\Big(i_0^{(i')}\Big)x_i^{(i')}.\end{aligned}$$

With the fact that for the leaders, $x_i = \rho_0 - z_i$ and the z-axis of $\Sigma_{i'}$ is parallel to i_0. Thus, we deduce that $\dot{\psi}_i = 0$.

Next we consider the following:

$$\begin{aligned}\dot{\psi}_i &= R_{i'}^{-1}\dot{R}(t_0 - t)R_{i'}(z_i - \rho_0) + R_{i'}^{-1}R(t_0 - t)R_{i'}\dot{z}_i \\ &= R_{i'}^{-1}\begin{bmatrix}-\sin(t - t_0) & \cos(t - t_0) & 0 \\ -\cos(t - t_0) & -\sin(t - t_0) & 0 \\ 0 & 0 & 0\end{bmatrix}\Big(z_i^{(i')} - \rho_0^{(i')}\Big) \\ &\quad - R_{i'}^{-1}R(t_0 - t)R\Big(\frac{\pi}{2}\Big)R_{i'}P(i_0)(y_i + \rho_0 - z_i) \\ &\quad + R_{i'}^{-1}R(t_0 - t)R_{i'}\left(\sum_{j\in\mathcal{N}_i^-(t)} k_{ji}(t)\zeta_j - \sum_{j\in\mathcal{N}_i^+(t)} k_{ij}(t)\zeta_i\right) \\ &= -R_{i'}^{-1}R(t_0 - t)R(\frac{\pi}{2})R_{i'}P(i_0)y_i + R_{i'}^{-1}R(t_0 - t)R_{i'} \\ &\quad \times \left(\sum_{j\in\mathcal{N}_i^-(t)} k_{ji}(t)\zeta_j - \sum_{j\in\mathcal{N}_i^+(t)} k_{ij}(t)\zeta_i\right).\end{aligned}$$

We define

$$\phi_i = R_{i'}^{-1}R(t_0 - t)R_{i'}\zeta_i$$

and

$$f_i(t) = -R_{i'}^{-1}R(t_0 - t)R\Big(\frac{\pi}{2}\Big)R_{i'}P(i_0)y_i.$$

For the leaders, we have $\dot{\psi}_i = 0$ and $\dot{\phi}_i = 0$. For the followers, it is obtained that

$$\begin{aligned}\dot{\phi}_i &= R_{i'}^{-1}\dot{R}(t_0 - t)R_{i'}\zeta_i + R_{i'}^{-1}R(t_0 - t)R_{i'}\dot{\zeta}_i \\ &= R_{i'}^{-1}\dot{R}(t_0 - t)R_{i'}\zeta_i + R_{i'}^{-1}R(t_0 - t)R_{i'} \\ &\quad \times \left(-R_{i'}^{-1}\hat{R}R_{i'}\zeta_i - \frac{1}{2}\zeta_i - \sum_{j\in\mathcal{N}_i^+(t)} k_{ij}(t)\big(z_j - z_i\big)\right) \\ &= R_{i'}^{-1}\dot{R}(t_0 - t)R_{i'}\zeta_i - R_{i'}^{-1}R(t_0 - t)\hat{R}R_{i'}\zeta_i - \frac{1}{2}\phi_i \\ &\quad - \sum_{j\in\mathcal{N}_i^+(t)} k_{ij}(t)\big(\psi_j - \psi_i\big) \\ &= -\frac{1}{2}\phi_i - \sum_{j\in\mathcal{N}_i^+(t)} k_{ij}(t)\big(\psi_j - \psi_i\big)\end{aligned}$$

and

$$\dot{\psi}_i = \sum_{j\in\mathcal{N}_i^-(t)} k_{ji}(t)\phi_j - \sum_{j\in\mathcal{N}_i^+(t)} k_{ij}(t)\phi_i + f_i.$$

Note that $\psi_i(0) = z_i(0)$ and $\phi_i(0) = \zeta_i(0)$. Let

$$\begin{cases} \psi^* = (I_N \otimes \gamma A)p + \mathbf{1}_N \otimes c \\ \phi^* = 0 \end{cases}$$

and apply the coordinate transformation $e_f = \psi_f - \psi_f^*$. Then we obtain

$$\begin{bmatrix} \dot{e}_f \\ \dot{\phi}_f \end{bmatrix} = \left(\begin{bmatrix} 0 & -L_{ff}^{\top}(t) \\ L_{ff}(t) & -\frac{1}{2}I_n \end{bmatrix} \otimes I_3 \right) \begin{bmatrix} e_f \\ \phi_f \end{bmatrix} + \begin{bmatrix} f_f \\ 0 \end{bmatrix}. \quad (31)$$

We have shown in Section IV that

$$\begin{bmatrix} \dot{e}_f \\ \dot{\phi}_f \end{bmatrix} = \left(\begin{bmatrix} 0 & -L_{ff}^{\top}(t) \\ L_{ff}(t) & -\frac{1}{2}I_n \end{bmatrix} \otimes I_3 \right) \begin{bmatrix} e_f \\ \phi_f \end{bmatrix}$$

is globally uniformly asymptotically stable. Moreover, from Lemma 6 we also obtain that y_i globally uniformly asymptotically converges to zero. Consequently, on the basis of Lemma 7, to complete the proof it only remains to verify that the condition (1) in Lemma 7 is satisfied.

Let

$$C(t) = \left(\begin{bmatrix} 0 & -L_{ff}^{\top}(t) \\ L_{ff}(t) & -\frac{1}{2}I_n \end{bmatrix} \otimes I_3 \right)$$

and

$$b(t) = \begin{bmatrix} f_f(t) \\ 0 \end{bmatrix}, \mu = \begin{bmatrix} e_f \\ \phi_f \end{bmatrix}.$$

For each $r > 0$, suppose

$$\left\| \begin{bmatrix} \mu(t_0) \\ y_f(t_0) \end{bmatrix} \right\| < r$$

then we know $\|\mu(t_0)\| < r$ and $\|y_f(t_0)\| < r$. The solution of (31) can be expressed by $\mu(t) = e^{\int_{t_0}^{t} C(\tau)d\tau}\mu(t_0) + \int_{t_0}^{t} e^{\int_{\tau}^{t} C(t')dt'} b(\tau)d\tau$. Take norm on both sides and we have

$$\|\mu(t)\| \leq \left\| e^{\int_{t_0}^{t} C(\tau)d\tau} \right\| \|\mu(t_0)\| + \int_{t_0}^{t} \left\| e^{\int_{\tau}^{t} C(t')dt'} \right\| \|b(\tau)\| d\tau.$$

Since the system (20) is exponentially stable, there must exist positive k and λ such that $\|e^{\int_{t_0}^{t} C(\tau)d\tau}\| \leq ke^{-\lambda(t-t_0)}$, which leads to the fact that

$$\|\mu(t)\| \leq ke^{-\lambda(t-t_0)}\|\mu(t_0)\| + \int_{t_0}^{t} ke^{-\lambda(t-\tau)}\|b(\tau)\|d\tau.$$

Note that every state $y_i(t)$ is a convex combination of $y_1(t_0), \ldots, y_N(t_0)$ [35, p. 78]. So it is valid that $\|y_i(t)\| < r$, and together with the fact that $\|f_i(t)\| \leq \|y_i(t)\|$, we can infer that $\|b(t)\|$ is upper bounded by a function $\bar{c}_y(r)$. Hence, we have

$$\begin{aligned} \|\mu(t)\| &\leq ke^{-\lambda(t-t_0)}\|\mu(t_0)\| + \bar{c}_y(r)\int_{t_0}^{t} ke^{-\lambda(t-\tau)}d\tau \\ &\leq k\|\mu(t_0)\| + \frac{k\bar{c}_y(r)}{\lambda} \leq kr + \frac{k\bar{c}_y(r)}{\lambda}. \end{aligned}$$

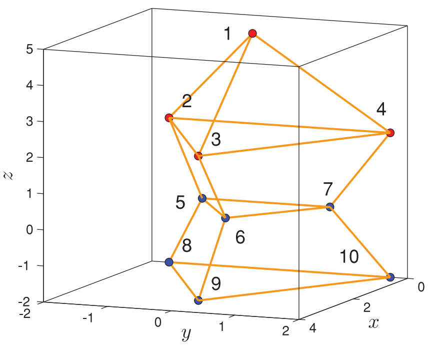

Fig. 6. Target configuration.

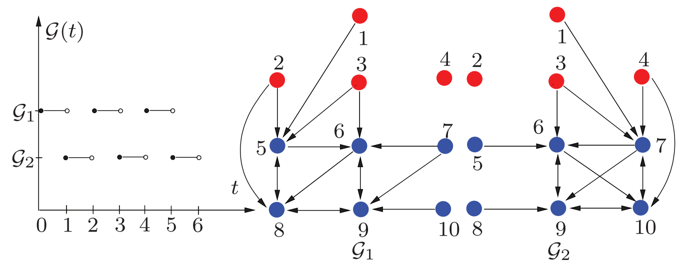

Fig. 7. Switching graph $\mathcal{G}(t)$ that switches between two graphs.

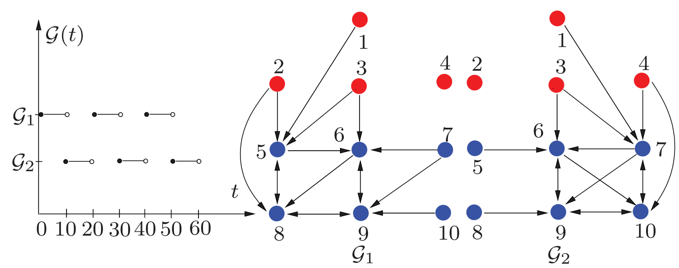

Fig. 8. Graphs $\mathcal{G}_1$ and $\mathcal{G}_2$ switch every 10 s.

Therefore, there exists $\bar{c}(r)$ such that

$$\left\| \begin{bmatrix} \mu(t) \\ y_f(t) \end{bmatrix} \right\| < \bar{c}(r).$$

Hence, ψ_i converges to $\gamma Ap_i + c$ globally uniformly asymptotically. Equivalently, z_i globally uniformly asymptotically converges to $R_{i'}^{-1}R(t - t_0)R_{i'}(\gamma Ap_i + c - \rho_0) + \rho_0$. Hence, the conclusion follows. ■

Remark 11: To meet Assumption 3, one sufficient condition is that the orientations of all local coordinate systems are consistent. However, this is not necessary. For instance, with extra edges for information exchange, Assumption 3 can be satisfied. Apart from edge $(j, i) \in \mathcal{E}$, by adding $(i, j), (k, j), (k, i) \in \mathcal{E}$, agent i manages to sense $z_j^i - z_i^i$ and $z_k^i - z_i^i$ while j can get $z_i^j - z_j^j$ and $z_k^j - z_j^j$. Then R_{ij} can be computed by solving the equation as below

$$\begin{cases} z_j^{(i)} - z_i^{(i)} = -R_{ij}\left(z_i^{(j)} - z_j^{(j)}\right) \\ z_j^{(i)} - z_i^{(i)} + R_{ij}\left(z_k^{(j)} - z_j^{(j)}\right) = z_k^{(i)} - z_i^{(i)}. \end{cases}$$

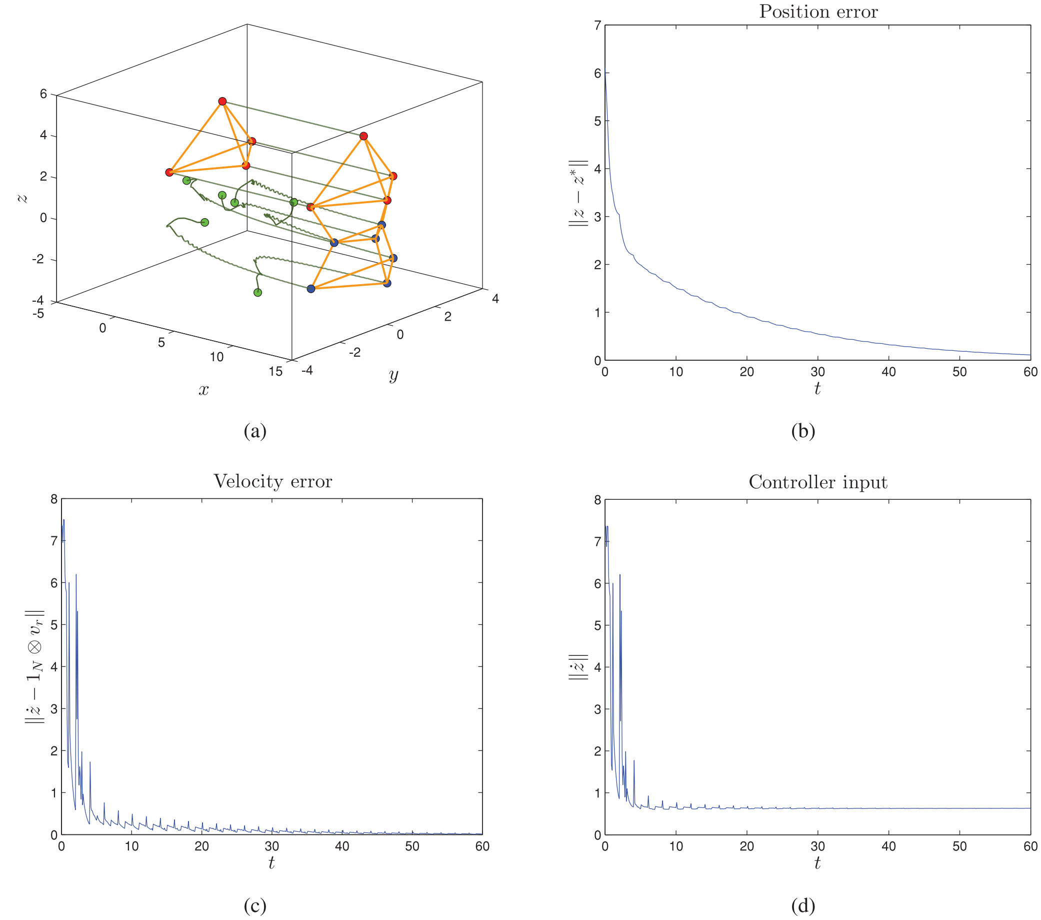

Fig. 9. (a) Trajectories of formation marching. (b) Error between the real position and the target position. (c) Error between the true velocity and the target velocity. (d) Norm of the control input.

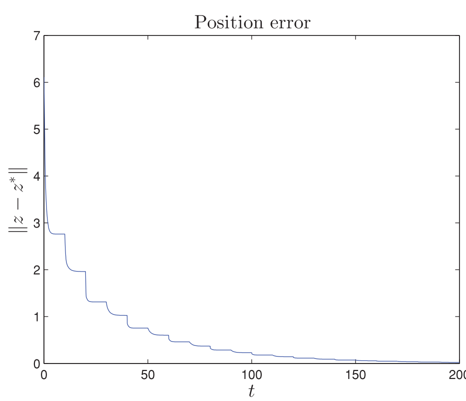

Fig. 10. Error between the real position and the target position for the case $T = 20$.

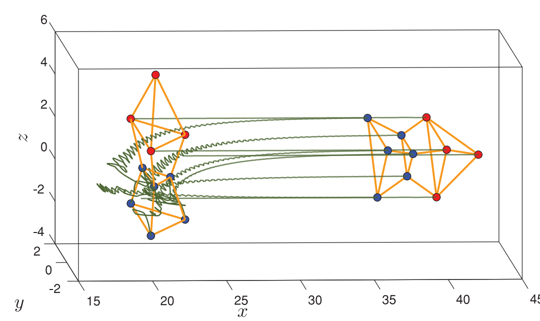

Fig. 11. Formation shape can be reconfigured by the leaders.

VI. SIMULATIONS

In this section, we present three simulation examples to illustrate our theoretical results.

We consider a system of four leaders which move in a similar formation and other six followers. The target configuration p is supposed to be the one in Fig. 6, where the leader set is $\mathcal{V}_l = \{1, \dots, 4\}$ and the follower set is $\mathcal{V}_f = \{5, \dots, 10\}$.

We draw the interaction graph $\mathcal{G}(t)$ used in the simulations in Fig. 7, and it can be checked that $\mathcal{G}(t)$ satisfies the two conditions in Theorems 2 and 3 by selecting the period as $T = 2$.

First, we carry out the simulations using the controller (4) for the leaders and (11) for the followers. A simulation result is plotted in Fig. 9, where Fig. 9(a) shows the trajectories of all the agents and the position error, velocity error, and controller input are plotted in Fig. 9(b)–(d), respectively. There are glitches in the signals in Fig. 9(c) and (d) since switching occurs during these time instants. But, we can still see from the results that the agents globally reach the target similar formation for the formation marching control.

Moreover, we change the switching signal in Fig. 7 such that $\mathcal{G}_1$ and $\mathcal{G}_2$ switch every 10 s, shown in Fig. 8. The position

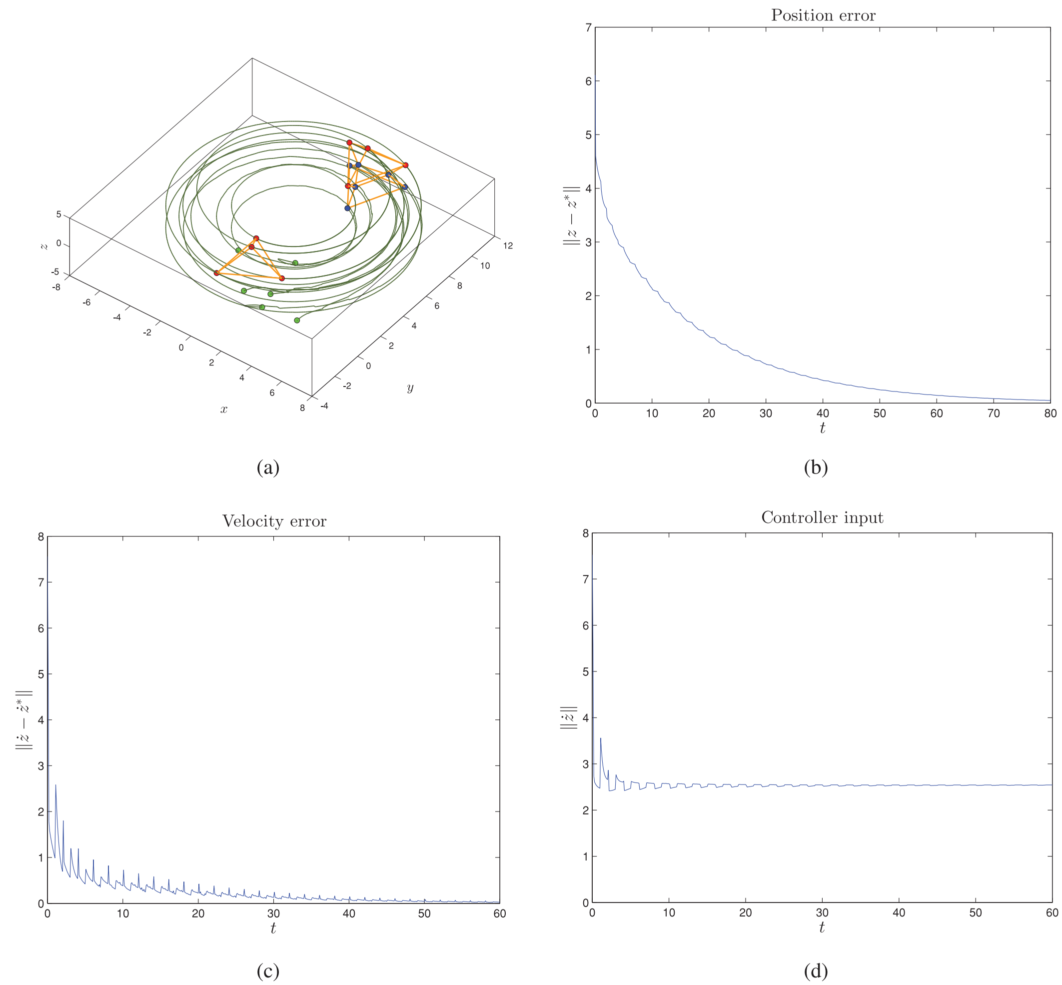

Fig. 12. (a) Trajectories of formation rotating. (b) Error between the real position and the target position. (c) Error between the true velocity and the target velocity. (d) Norm of the control input.

error for this situation is recorded in Fig. 10, from which we can see that larger period T indicates slower convergence.

Second, we consider a scenario that all the agents have reached the target similar formation for the formation marching control as shown in Fig. 9(a). Then we impose extra force on the leaders to change the leaders' formation shape and also use the same controller (11) for the followers. A simulation result is given in Fig. 11, which demonstrates that the formation shape of the whole group can be reconfigured by the leaders while the followers only act as dummies.

Third, we adopt the control law (7) for the leaders and (28) for the followers. A simulation result is plotted in Fig. 12, where Fig. 12(a) shows the trajectories of all the agents and the position error, velocity error, and controller input are plotted in Fig. 12(b)–(d), respectively. We can see that a similar formation is realized for the formation rotating control.

VII. Conclusion

This paper investigates the two formation control problems for a leader–follower network in the three dimensions, that is, formation marching control problem and formation rotating control problem. By exchanging an auxiliary state via communication, fully distributed control laws are developed for both scenarios. Moreover, the same conditions are obtained to guarantee global convergence for both problems.

One future study is to extend the control laws in this paper to second-order cases or more complex agent dynamics. One possible approach is to take advantage of the backstepping philosophy. Specifically, design the acceleration input such that the velocity signal in the second-order case converges to the desired velocity signal produced by the proposed control laws in this paper. Another future study is to consider controller design with smooth velocities even in the presence of topology switching, which seems to be interesting and practical.

Appendix

Proof of Lemma 2: We denote $U = \mathcal{V}\backslash\mathcal{R}$ and relabel the nodes in $\mathcal{R}$ and $\mathcal{U}$ consecutively. As a result the matrix L is transformed to the form

$$L' := \begin{bmatrix} L_{11} & L_{12} \\ L_{21} & L_{22} \end{bmatrix}$$

where L_{11} correspond to the nodes in $\mathcal{R}$ and L_{22} correspond to the nodes in $\mathcal{U}$. Thus, we have

$$\begin{bmatrix} L_{21} & L_{22} \end{bmatrix}\mathbf{1} = 0, \ \begin{bmatrix} L_{21} & L_{22} \end{bmatrix}P\xi = 0$$
$$\begin{bmatrix} L_{21} & L_{22} \end{bmatrix}P\zeta = 0, \begin{bmatrix} L_{21} & L_{22} \end{bmatrix}P\eta = 0.$$

Due to that ξ, ζ, and η are generic, we know that the rows of L_{22} lie in an $(n-4)$-dimensional linear subspace. Since $m < 4$, we can infer that L_{22} is not of full row rank, which means that $\det(L_{\mathcal{R}}) = 0$ for any $L \in \{L \in \mathcal{L}(\mathcal{G}) : L\xi = 0, L\zeta = 0, L\eta = 0\}$. ■

We summarize two results in [20] for proving Theorem 1.

Lemma 8 [20]: Consider a spanning 4-tree $\mathcal{T} = (\mathcal{V}, \mathcal{E})$ with n nodes and generic $\xi, \zeta, \eta \in \mathbb{R}^n$. Then for all $L \in \{L \in \mathcal{L}(\mathcal{T}) : L\xi = 0, L\zeta = 0, L\eta = 0\}$, all principal minors of $L_{\mathcal{R}}$ are nonzero, where $\mathcal{R}$ is the root set.

Lemma 9 [20]: Consider a root set $R = \{r_1, r_2, \ldots, r_k\}$ such that any node in $\mathcal{V}\backslash\mathcal{R}$ is k-reachable from $\mathcal{R}$. Then for the Laplacian L of $\mathcal{G}$ with almost all weights w_{ij}s:

1) all the principal minors of $L_{\mathcal{R}}$ are nonzero;
2) $\det(M) \neq 0$ where M is a sub-matrix of L by deleting the rows corresponding to the k roots and any k columns.

Proof of Theorem 1: (1) $\Longrightarrow$ (2) If (1) holds, we add edges $(r_k, r_1), (r_k, r_2), (r_k, r_3), (r_k, r_4)$ for $k = 5, \ldots, m$ and thus construct a new graph, denoted by $\mathcal{G}'$, which has a spanning 4-tree as its subgraph with the root set $\mathcal{R}' = \{r_1, r_2, r_3, r_4\}$. We denote this spanning 4-tree by $\mathcal{T}$ and thus by Lemma 8 we know that all the principal minors of $L_{\mathcal{R}'}$ are nonzero for any $L \in \{L \in \mathcal{L}(\mathcal{T}) : L\xi = 0, L\zeta = 0, L\eta = 0\}$.

Notice that the difference between $L \in \{L \in \mathcal{L}(\mathcal{G}') : L\xi = 0, L\zeta = 0, L\eta = 0\}$ and $L' \in \{L' \in \mathcal{L}(\mathcal{T}) : L'\xi = 0, L'\zeta = 0, L'\eta = 0\}$ is that some nonzero weights in L become zero in L'. According to the fact that either a polynomial is zero or it is not zero almost everywhere, we can infer that for almost all $L \in \{L \in \mathcal{L}(\mathcal{G}') : L\xi = 0, L\zeta = 0, L\eta = 0\}$, all the principal minors of $L_{\mathcal{R}'}$ are nonzero. Moreover, since $\mathcal{R}' \subset \mathcal{R}$, after relabeling the nodes properly, it is obtained that for almost all $L \in \{L \in \mathcal{L}(\mathcal{G}) : L\xi = 0, L\zeta = 0, L\eta = 0\}$, all the principal minors of $L_{\mathcal{R}}$ are nonzero.

(2) $\Longrightarrow$ (1) Suppose that there exists a node $i \notin \mathcal{R}$ such that after deleting three nodes, without loss of generality, say $\{1, 2, 3\}$, i is not reachable from $\mathcal{R}$. Define a set U including the nodes that are not reachable from $\mathcal{R}$ after removing nodes 1, 2, and 3. Denote $\bar{\mathcal{U}} = \mathcal{V} - \mathcal{U} - \{1, 2, 3\}$. Note that $\bar{\mathcal{U}}$ cannot be empty since there are m nodes in $\mathcal{R}$. Moreover, it is true that there is no edge leading from a node in $\bar{\mathcal{U}}$ to a node in $\mathcal{U}$. After relabeling the nodes, the matrix L becomes the one with the structure as

$$L' := \begin{bmatrix} L_{11} & L_{12} & L_{13} \\ L_{21} & L_{22} & 0 \\ L_{31} & L_{32} & L_{33} \end{bmatrix}$$

where L_{11} correspond to $\{1, 2, 3\}$, L_{22} correspond to the nodes in $\mathcal{U}$, and L_{33} correspond to the nodes in $\bar{\mathcal{U}}$. Thus, it is known that

$$\begin{bmatrix} L_{21} & L_{22} & 0 \end{bmatrix}\mathbf{1} = 0, \ \begin{bmatrix} L_{21} & L_{22} & 0 \end{bmatrix}P\xi = 0$$
$$\begin{bmatrix} L_{21} & L_{22} & 0 \end{bmatrix}P\zeta = 0, \ \begin{bmatrix} L_{21} & L_{22} & 0 \end{bmatrix}P\eta = 0.$$

Since ξ, ζ, and η are generic, the rows of $[L_{21}\ L_{22}]$ lie in an $(n - |\bar{\mathcal{U}}| - 4)$-dimensional linear subspace. Moreover, $[L_{21}\ L_{22}]$ has $n - |\bar{\mathcal{U}}| - 3$ rows. Thus, we can infer that $[L_{21}\ L_{22}]$ is not of full row rank, which means $\det(L_{\mathcal{R}}) = 0$ for any $L \in \{L \in \mathcal{L}(\mathcal{G}) : L\xi = 0, L\zeta = 0, L\eta = 0\}$. ■

Proof of Lemma 3: Note that each $L(i, :) \in \Omega_i(\mathcal{F})$ lies in a 1-D linear subspace. The proof of Theorem 1 indicates that if the linear subspace formed by all possible $L(i, :)$s in Θ_i contains the 1-D linear subspace formed by all possible $L'(i, :)$s in $\Omega_i(\mathcal{F})$, then for almost all L, all principal minors of $L_{\mathcal{R}}$ are nonzero. ■

REFERENCES

[1] R. M. Murray, "Recent research in cooperative control of multivehicle systems," *J. Dyn. Syst. Meas. Control*, vol. 129, no. 5, pp. 571–583, 2007.

[2] Z. Lin, B. Francis, and M. Maggiore, "Necessary and sufficient graphical conditions for formation control of unicycles," *IEEE Trans. Autom. Control*, vol. 50, no. 1, pp. 121–127, Jan. 2005.

[3] B. D. O. Anderson, C. Yu, B. Fidan, and J. M. Hendrickx, "Rigid graph control architectures for autonomous formations," *IEEE Control Syst. Mag.*, vol. 28, no. 6, pp. 48–63, Dec. 2008.

[4] Y.-H. Chang, C.-W. Chang, C.-L. Chen, and C.-W. Tao, "Fuzzy sliding-mode formation control for multirobot systems: Design and implementation," *IEEE Trans. Syst., Man, Cybern. B, Cybern.*, vol. 42, no. 2, pp. 444–457, Apr. 2012.

[5] V. Gazi and K. M. Passino, "Stability analysis of social foraging swarms," *IEEE Trans. Syst., Man, Cybern. B, Cybern.*, vol. 34, no. 1, pp. 539–557, Feb. 2004.

[6] W. Dong, "Flocking of multiple mobile robots based on backstepping," *IEEE Trans. Syst., Man, Cybern. B, Cybern.*, vol. 41, no. 2, pp. 414–424, Apr. 2011.

[7] M. Deghat, B. D. O. Anderson, and Z. Lin, "Combined flocking and distance-based shape control of multi-agent formations," *IEEE Trans. Autom. Control*, vol. 61, no. 7, pp. 1824–1837, Jul. 2016.

[8] Y. Cao, W. Ren, and M. Egerstedt, "Distributed containment control with multiple stationary or dynamic leaders in fixed and switching directed networks," *Automatica*, vol. 48, no. 8, pp. 1586–1597, 2012.

[9] X. Wang, S. Li, and P. Shi, "Distributed finite-time containment control for double-integrator multiagent systems," *IEEE Trans. Cybern.*, vol. 44, no. 9, pp. 1518–1528, Sep. 2014.

[10] H. Su and M. Z. Q. Chen, "Multi-agent containment control with input saturation on switching topologies," *IET Control Theory Appl.*, vol. 9, no. 3, pp. 399–409, Feb. 2015.

[11] X. Wang, W. Ni, and X. Wang, "Leader-following formation of switching multirobot systems via internal model," *IEEE Trans. Syst., Man, Cybern. B, Cybern.*, vol. 42, no. 3, pp. 817–826, Jun. 2012.

[12] G. C. Chasparis and J. S. Shamma, "Network formation: Neighborhood structures, establishment costs, and distributed learning," *IEEE Trans. Cybern.*, vol. 43, no. 6, pp. 1950–1962, Dec. 2013.

[13] A. N. Bishop, M. Deghat, B. D. O. Anderson, and Y. Hong, "Distributed formation control with relaxed motion requirements," *Int. J. Robust Nonlin. Control*, vol. 25, no. 17, pp. 3210–3230, 2015.

[14] Z. Han, L. Wang, Z. Lin, and R. Zheng, "Formation control with size scaling via a complex Laplacian-based approach," *IEEE Trans. Cybern.*, vol. 46, no. 10, pp. 2348–2359, Oct. 2016.

[15] X. Dong, L. Han, Q. Li, and Z. Ren, "Time-varying formation control for double-integrator multi-agent systems with jointly connected topologies," *Int. J. Syst. Sci.*, vol. 47, no. 16, pp. 3829–3838, 2016.

[16] X. Dong, Y. Zhou, Z. Ren, and Y. Zhong, "Time-varying formation control for unmanned aerial vehicles with switching interaction topologies," *Control Eng. Pract.*, vol. 46, pp. 26–36, Jan. 2016.

[17] K.-K. Oh, M.-C. Park, and H.-S. Ahn, "A survey of multi-agent formation control," *Automatica*, vol. 53, pp. 424–440, Mar. 2015.

[18] Z. Lin, L. Wang, Z. Han, and M. Fu, "Distributed formation control of multi-agent systems using complex Laplacian," *IEEE Trans. Autom. Control*, vol. 59, no. 7, pp. 1765–1777, Jul. 2014.

[19] Z. Lin, L. Wang, Z. Han, and M. Fu, "A graph Laplacian approach to coordinate-free formation stabilization for directed networks," *IEEE Trans. Autom. Control*, vol. 61, no. 5, pp. 1269–1280, May 2016.

[20] Z. Lin, L. Wang, Z. Chen, M. Fu, and Z. Han, "Necessary and sufficient graphical conditions for affine formation control," *IEEE Trans. Autom. Control*, vol. 61, no. 10, pp. 2877–2891, Oct. 2016.

[21] H. Coxeter, *Introduction to Geometry*. John Wiley & Sons, Inc., 1969.

[22] T. Han, Z. Lin, and M. Fu, "Three-dimensional formation merging control under directed and switching topologies," *Automatica*, vol. 58, pp. 99–105, Aug. 2015.

[23] R. Sepulchre, D. A. Paley, and N. E. Leonard, “Stabilization of planar collective motion with limited communication,” *IEEE Trans. Autom. Control*, vol. 53, no. 3, pp. 706–719, Apr. 2008.
[24] Z. Chen and H.-T. Zhang, “A remark on collective circular motion of heterogeneous multi-agents,” *Automatica*, vol. 49, no. 5, pp. 1236–1241, 2013.
[25] P. Li, K. Qin, and M. Shi, “Distributed robust H_∞ rotating consensus control for directed networks of second-order agents with mixed uncertainties and time-delay,” *Neurocomputing*, vol. 148, pp. 332–339, Jan. 2015.
[26] P. Lin and Y. Jia, “Distributed rotating formation control of multi-agent systems,” *Syst. Control Lett.*, vol. 59, no. 10, pp. 587–595, 2010.
[27] P. Lin, K. Qin, Z. Li, and W. Ren, “Collective rotating motions of second-order multi-agent systems in three-dimensional space,” *Syst. Control Lett.*, vol. 60, no. 6, pp. 365–372, 2011.
[28] S. J. Gortler, A. D. Healy, and D. P. Thurston, “Characterizing generic global rigidity,” *Amer. J. Math.*, vol. 132, no. 4, pp. 897–939, 2010.
[29] J.-M. Dion, C. Commault, and J. van der Woude, “Generic properties and control of linear structured systems: A survey,” *Automatica*, vol. 39, no. 7, pp. 1125–1144, 2003.
[30] S. Mou, A. S. Morse, M. A. Belabbas, and B. D. O. Anderson, “Undirected rigid formations are problematic,” in *Proc. 53rd IEEE Conf. Decis. Control*, Los Angeles, CA, USA, 2014, pp. 637–642.
[31] S. Mou, M. Cao, and A. S. Morse, “Target-point formation control,” *Automatica*, vol. 61, pp. 113–118, Nov. 2015.
[32] B. D. O. Anderson, “Exponential stability of linear equations arising in adaptive identification,” *IEEE Trans. Autom. Control*, vol. 22, no. 1, pp. 83–88, Feb. 1977.
[33] Z. Lin, T. Han, R. Zheng, and M. Fu, “Distributed localization for 2-D sensor networks with bearing-only measurements under switching topologies,” *IEEE Trans. Signal Process.*, vol. 64, no. 23, pp. 6345–6359, Dec. 2016.
[34] E. Panteley and A. Loría, “Growth rate conditions for uniform asymptotic stability of cascaded time-varying systems,” *Automatica*, vol. 37, no. 3, pp. 453–460, 2001.
[35] Z. Lin, *Distributed Control and Analysis of Coupled Cell Systems*. Saarbrücken, Germany: VDM-Verlag, 2008.

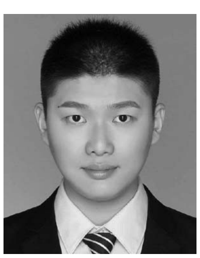

Tingrui Han received the bachelor’s degree in automation from Zhejiang University, Hangzhou, China, in 2012, where he is currently pursuing the Ph.D. degree in control theory and control engineering with the College of Electrical Engineering.

His current research interests include multiagent systems, networked control, and distributed algorithms.

Zhiyun Lin (SM’10) received the bachelor’s degree in electrical engineering from Yanshan University, Qinhuangdao, China, in 1998, the master’s degree in electrical engineering from Zhejiang University, Hangzhou, China, in 2001, and the Ph.D. degree in electrical and computer engineering from the University of Toronto, Toronto, ON, Canada, in 2005.

He is currently a Professor with the School of Automation, Hangzhou Dianzi University, Hangzhou. Preceding to this position, he held a Professor position with Zhejiang University from 2007 to 2016, and a Post-Doctoral Fellow position with the University of Toronto from 2005 to 2007. He held a Visiting Professor positions at several universities including the Australian National University, Canberra, ACT, Australia, the University of Cagliari, Cagliari, Italy, the University of Newcastle, Callaghan, NSW, Australia, the University of Technology Sydney, Ultimo, NSW, Australia, and Yale University, New Haven, CT, USA. His current research interests include distributed control, estimation and optimization, cooperative control of multiagent systems, hybrid control system theory, and robotics.

Dr. Lin is currently an Associate Editor for the IEEE CONTROL SYSTEMS LETTERS, *Hybrid Systems: Nonlinear Analysis*, and the *International Journal of Wireless and Mobile Networking*.

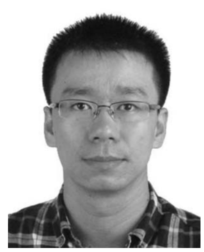

Ronghao Zheng received the bachelor’s degree in electrical engineering and the master’s degree in control theory and control engineering from Zhejiang University, Hangzhou, China, in 2007 and 2010, and the Ph.D. degree in mechanical and biomedical engineering from the City University of Hong Kong, Hong Kong, in 2014.

He is currently with the College of Electrical Engineering, Zhejiang University. His current research interest includes distributed algorithms and control, especially, the coordination of networked mobile robot teams with applications in automated systems and security.

Minyue Fu (F’03) received the bachelor’s degree in electrical engineering from the University of Science and Technology of China, Hefei, China, in 1982, and the M.S. and Ph.D. degrees in electrical engineering from the University of Wisconsin-Madison, Madison, WI, USA, in 1983 and 1987, respectively.

From 1987 to 1989, he served as an Assistant Professor with the Department of Electrical and Computer Engineering, Wayne State University, Detroit, MI, USA. He joined the Department of Electrical and Computer Engineering, University of Newcastle, Callaghan, NSW, Australia, in 1989, where he is currently a Chair Professor of Electrical Engineering. He was a Visiting Associate Professor with the University of Iowa, Iowa City, IA, USA, from 1995 to 1996, a Senior Fellow/Visiting Professor with Nanyang Technological University, Singapore, in 2002, and a Visiting Professor with Tokyo University, Bunkyo, Tokyo, in 2003. He has held a ChangJiang Visiting Professorship with Shandong University, Jinan, China, a Visiting Professorship with South China University of Technology, Guangzhou, China, and a Qian-Ren Professorship with Zhejiang University, Hangzhou, China. His current research interests include control systems, signal processing and communications, networked control systems, smart electricity networks, and super-precision positioning control systems.

Dr. Fu has been an Associate Editor for the IEEE TRANSACTIONS ON AUTOMATIC CONTROL, *Automatica*, the IEEE TRANSACTIONS ON SIGNAL PROCESSING, and the *Journal of Optimization and Engineering*.